Electronic Supplementary Information (ESI)

Structural and Anionic Effects of Microcrystalline Zn-CPs on 4-Nitrophenol Sensing Performances

Hyemin Lee[1], Min-Yeong Kim*[,2], and Haeri Lee*[,1]

[1]Department of Chemistry, Hannam University, Daejeon, 34054, Republic of Korea

[2]Department of Electrochemistry, Korea Institute of Materials Science (KIMS), Changwon, 51508, Republic of Korea

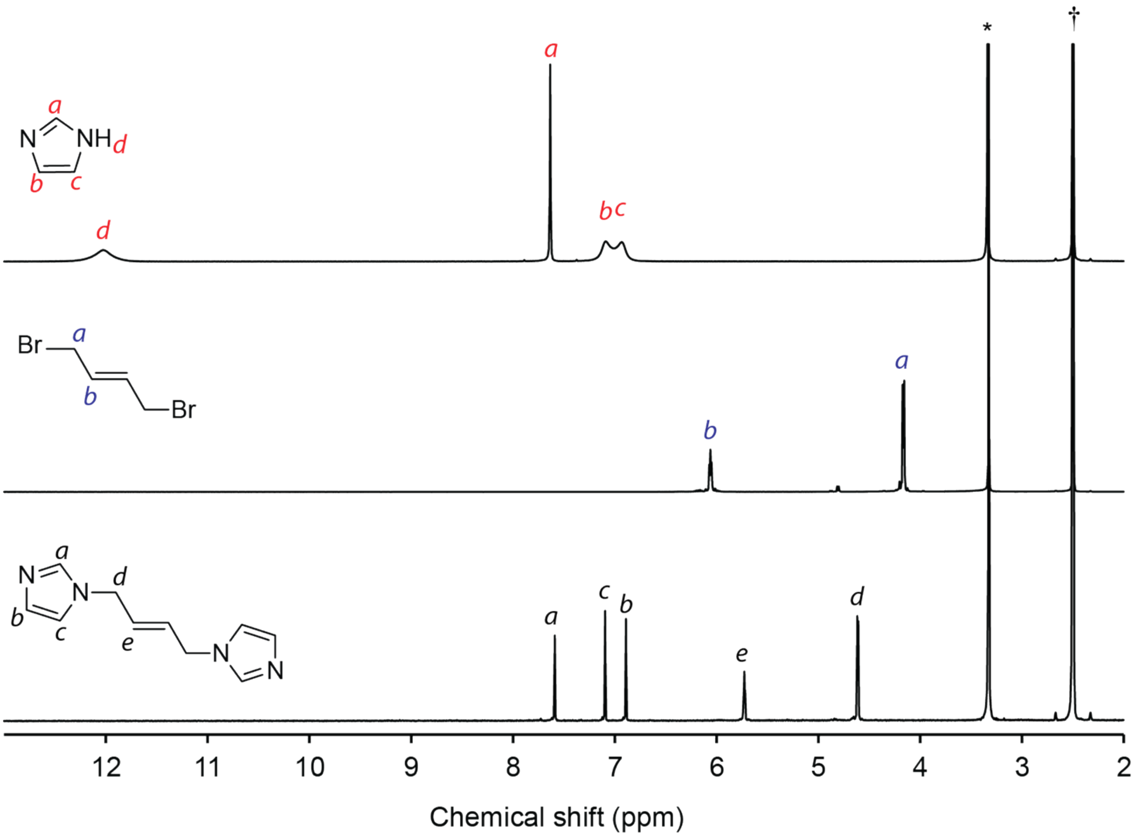

Figure S1. ^{1}H NMR spectrum for starting materials and **L** in DMSO-d_6 ($^\dagger CD_2HSOCD_2H$, $^*H_2O$).

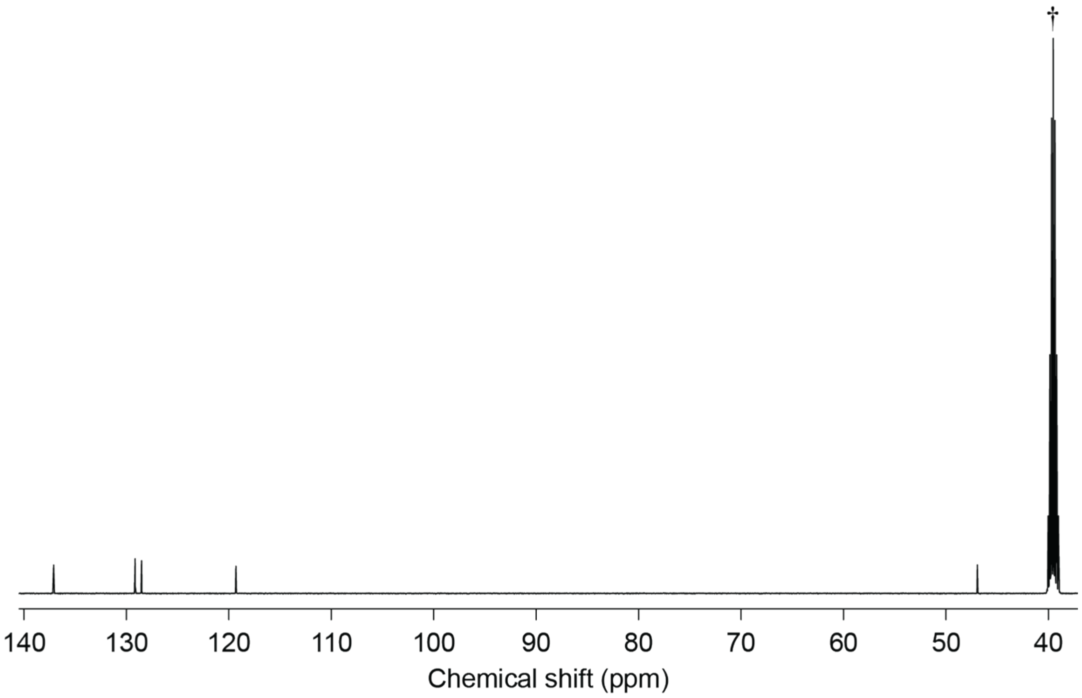

Figure S2. ^{13}C NMR spectrum for **L** in DMSO-d_6 ($^{\dagger}CD_2HSOCD_2H$, $^{*}H_2O$).

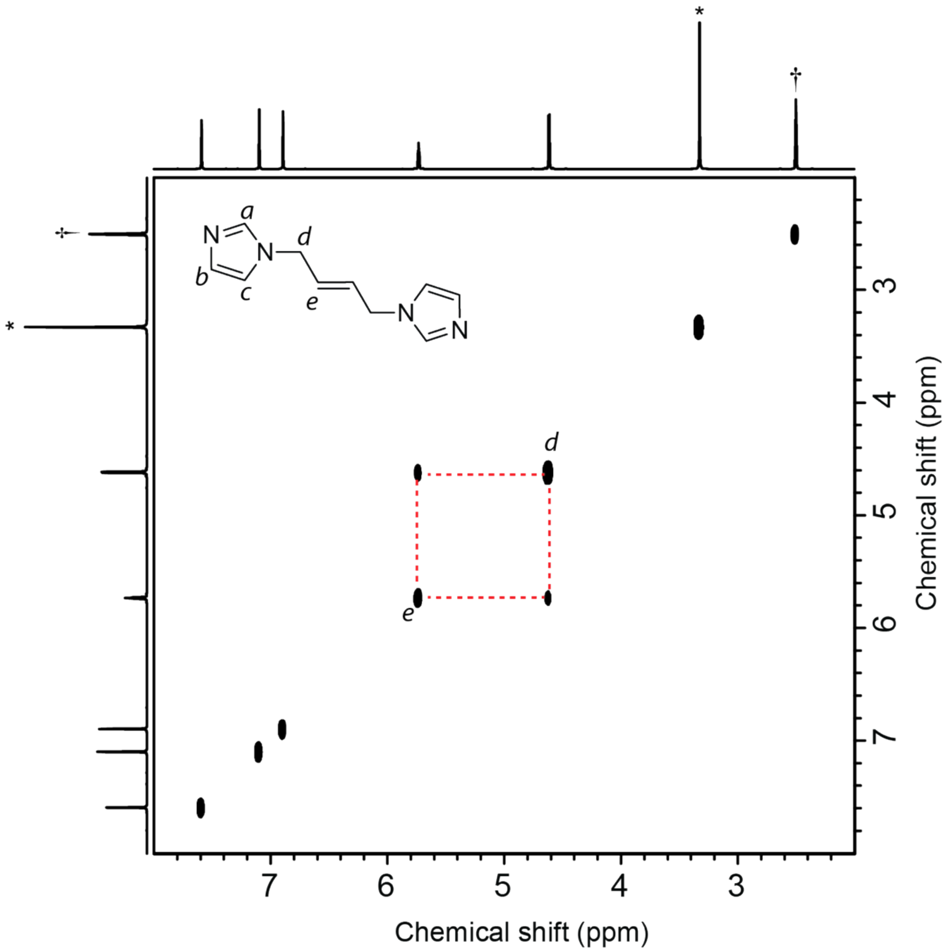

Figure S3. ^{1}H-^{1}H COSY spectrum for **L** in DMSO-d_6 ($^†CD_2HSOCD_2H$, $*H_2O$).

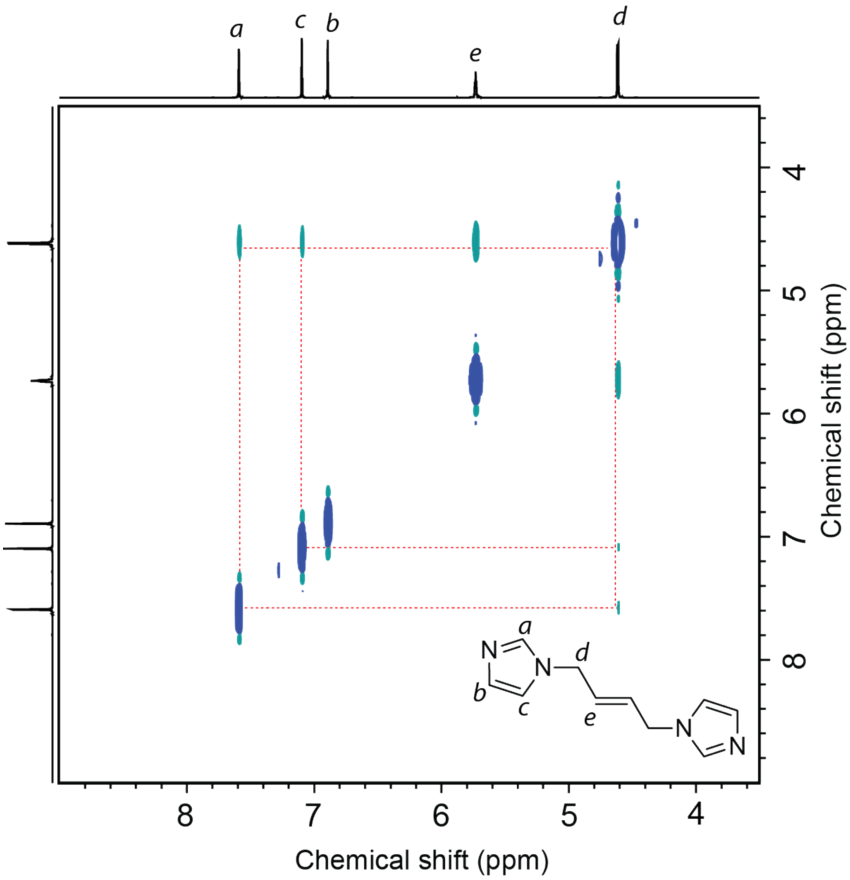

Figure S4. ^{1}H-^{1}H NOESY spectrum for **L** in DMSO-d_6.

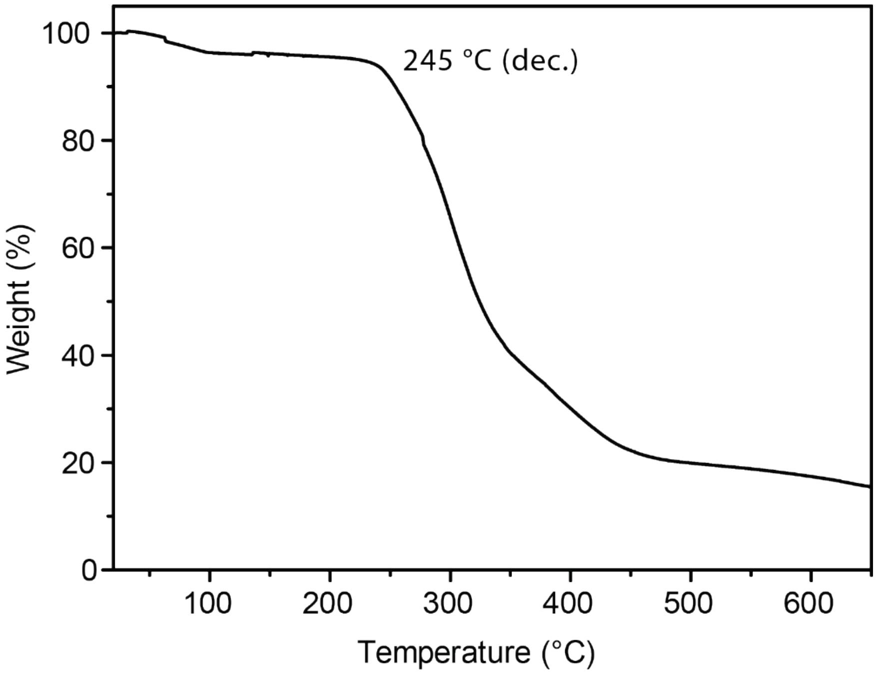

Figure S5. TG analysis for **L**.

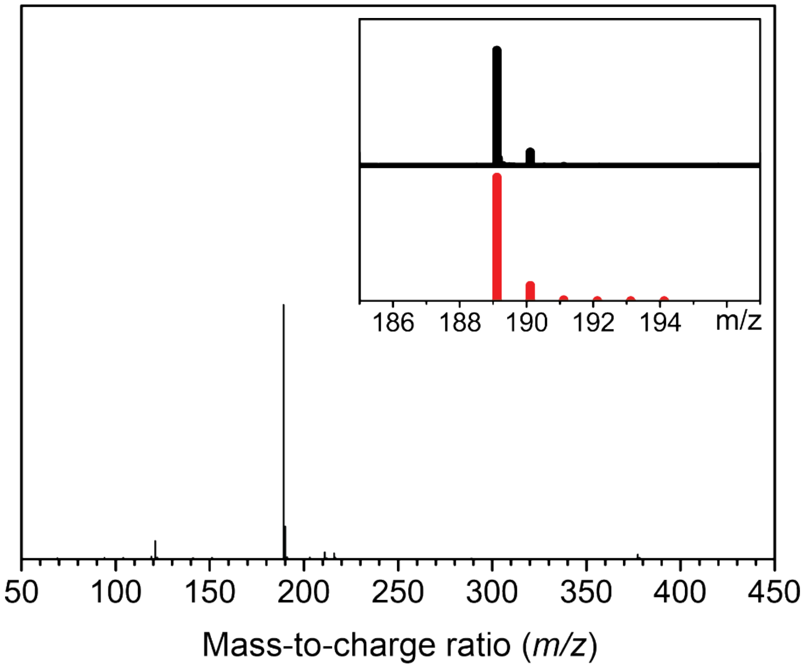

Figure S6. High-resolution ESI-Mass spectrum for **L**, *m/z* 189.1140 (black, inset) and calcd for $[C_{10}H_{12}N_2 + H^+]^+$ = 189.1140 (red, inset).

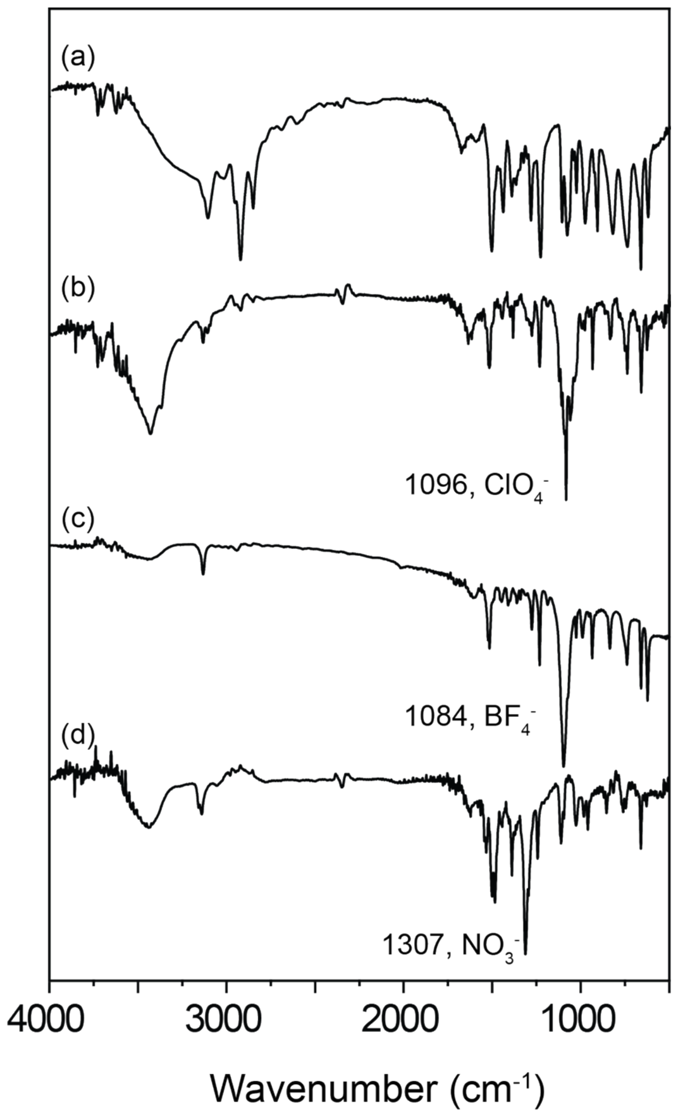

Figure S7. FT-IR spectra for **L** (a), $[Zn\mathbf{L}_3]_n(ClO_4)_{2n}$ (b), $[Zn\mathbf{L}_3]_n(BF_4)_{2n}$ (c), and $[Zn_2(NO_3)_4\mathbf{L}_3]_n$ (d).

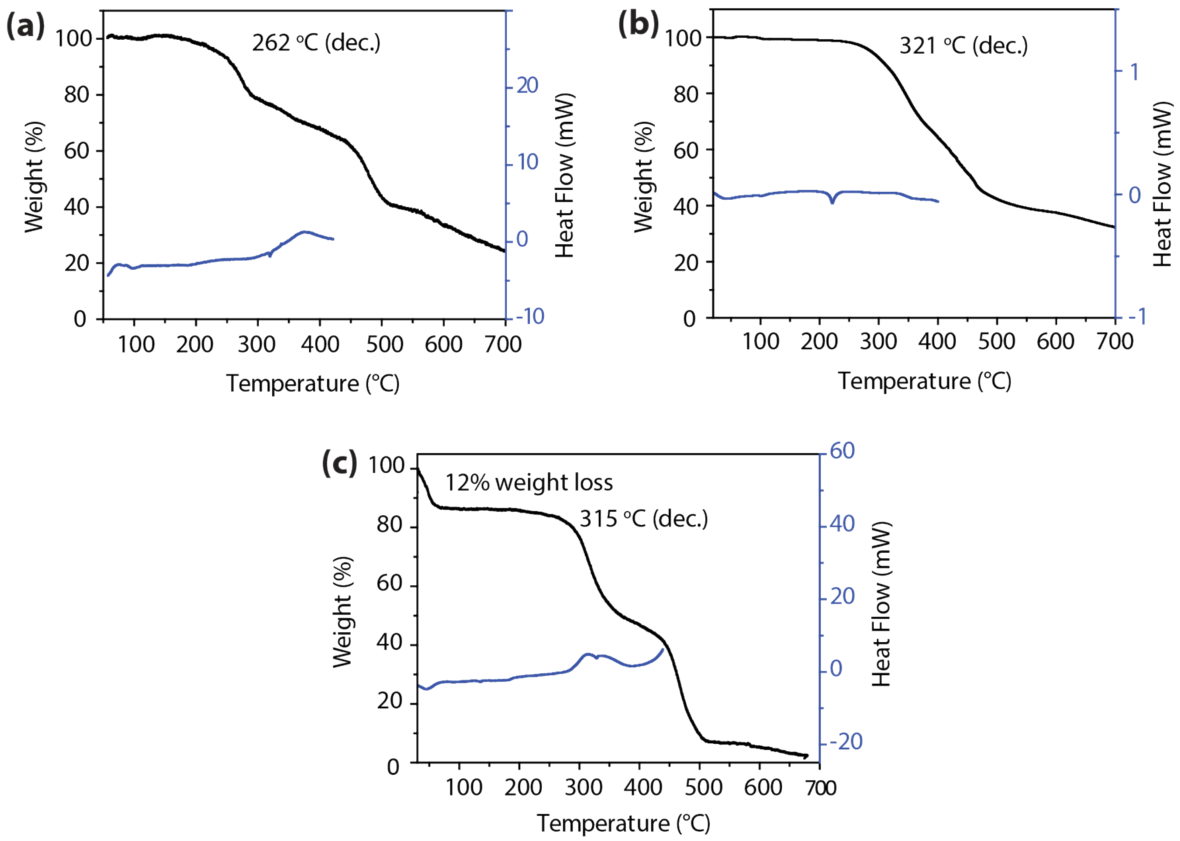

Figure S8. TG analyses and DSC curves for $[Zn\mathbf{L}_3]_n(ClO_4)_{2n}$ (a), $[Zn\mathbf{L}_3]_n(BF_4)_{2n}$ (b), and $[Zn_2(NO_3)_4\mathbf{L}_3]_n$ (c). For $[Zn_2(NO_3)_4\mathbf{L}_3]_n$, 12% weight loss in a range of 25 to 50°C refers to the evaporation of $CHCl_3$ which is the mother liquid for crystallization.

Refinement Details

Most disagreeable reflections were omitted by OMIT instruction.

For $[Zn_2(NO_3)_4\mathbf{L}_3]_n$, disordered solvate molecules were squeezed out by Platon.[1]

```
# SQUEEZE RESULTS (Version = 140621)
# Note: Data are Listed for all Voids in the P1 Unit Cell
# i.e. Centre of Gravity, Solvent Accessible Volume,
# Recovered number of Electrons in the Void and
# Details about the Squeezed Material
loop_
  _platon_squeeze_void_nr
  _platon_squeeze_void_average_x
  _platon_squeeze_void_average_y
  _platon_squeeze_void_average_z
  _platon_squeeze_void_volume
  _platon_squeeze_void_count_electrons
  _platon_squeeze_void_content
   1  0.000  0.000  0.500        121         32 ' '
```

Table S1. Selected bond lengths and angles for $[Zn\mathbf{L}_3]_n(BF_4)_{2n}$, $[Zn\mathbf{L}_3]_n(ClO_4)_{2n}$, and $[Zn_2(NO_3)_4\mathbf{L}_3]_n$

$[Zn\mathbf{L}_3]_n(BF_4)_{2n}$		$[Zn\mathbf{L}_3]_n(ClO_4)_{2n}$		$[Zn_2(NO_3)_4\mathbf{L}_3]_n$	
Zn(1)-N(1)#1	2.192(3)	Zn(1)-N(2)#1	2.1949(13)	Zn(1)-N(1)	1.9809(18)
Zn(1)-N(1)#2	2.192(3)	Zn(1)-N(2)#2	2.1949(13)	Zn(1)-N(3)	1.9984(17)
Zn(1)-N(1)#3	2.192(3)	Zn(1)-N(2)#3	2.1949(13)	Zn(1)-N(5)	2.0088(18)
Zn(1)-N(1)#4	2.192(3)	Zn(1)-N(2)#4	2.1949(13)	Zn(1)-O(1)	2.0730(17)
Zn(1)-N(1)#5	2.192(3)	Zn(1)-N(2)#5	2.1949(13)	N(1)-Zn(1)-N(3)	115.21(7)
Zn(1)-N(1)	2.192(3)	Zn(1)-N(2)	2.1949(13)	N(1)-Zn(1)-N(5)	116.98(7)
N(1)#1-Zn(1)-N(1)#2	180.00(9)	N(2)#1-Zn(1)-N(2)#2	92.43(5)	N(3)-Zn(1)-N(5)	121.92(7)
N(1)#1-Zn(1)-N(1)#3	91.96(10)	N(2)#1-Zn(1)-N(2)#3	87.57(5)	N(1)-Zn(1)-O(1)	102.89(8)
N(1)#2-Zn(1)-N(1)#3	88.04(10)	N(2)#2-Zn(1)-N(2)#3	180.00(6)	N(3)-Zn(1)-O(1)	102.99(8)
N(1)#1-Zn(1)-N(1)#4	88.04(10)	N(2)#1-Zn(1)-N(2)#4	87.57(5)	N(5)-Zn(1)-O(1)	88.70(7)
N(1)#2-Zn(1)-N(1)#4	91.96(10)	N(2)#2-Zn(1)-N(2)#4	87.57(5)		
N(1)#3-Zn(1)-N(1)#4	180.00(11)	N(2)#3-Zn(1)-N(2)#4	92.43(5)		
N(1)#1-Zn(1)-N(1)#5	91.96(10)	N(2)#1-Zn(1)-N(2)#5	92.43(5)		
N(1)#2-Zn(1)-N(1)#5	88.04(10)	N(2)#2-Zn(1)-N(2)#5	92.43(5)		
N(1)#3-Zn(1)-N(1)#5	91.96(10)	N(2)#3-Zn(1)-N(2)#5	87.57(5)		
N(1)#4-Zn(1)-N(1)#5	88.04(10)	N(2)#4-Zn(1)-N(2)#5	180.00(12)		
N(1)#1-Zn(1)-N(1)	88.04(10)	N(2)#1-Zn(1)-N(2)	180		
N(1)#2-Zn(1)-N(1)	91.96(10)	N(2)#2-Zn(1)-N(2)	87.57(5)		
N(1)#3-Zn(1)-N(1)	88.04(10)	N(2)#3-Zn(1)-N(2)	92.43(5)		
N(1)#4-Zn(1)-N(1)	91.96(10)	N(2)#4-Zn(1)-N(2)	92.43(5)		
N(1)#5-Zn(1)-N(1)	180	N(2)#5-Zn(1)-N(2)	87.57(5)		

#1 y,-x+y,-z+2 #2 -y,x-y,z #3 x-y,x,-z+2 #4 -x+y,-x,z #5 -x,-y,-z+2

#1 -x,-y,-z #2 x-y,x,-z #3 -x+y,-x,z #4 -y,x-y,z #5 y,-x+y,-z

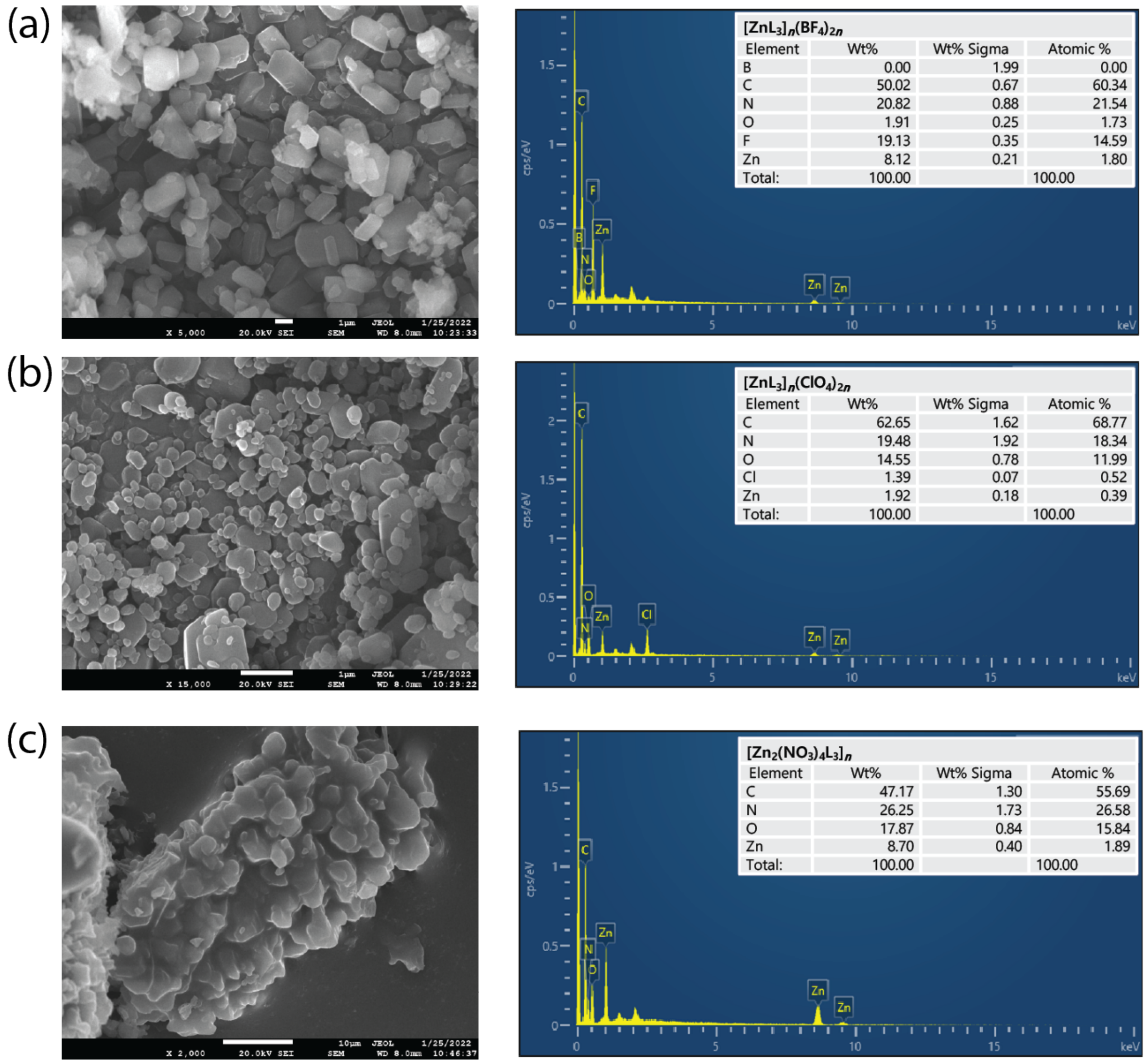

Figure S9. SEM images and EDS data for microcrystals were obtained after the deposition on SPEC working electrode from the dispersion in an aqueous solution for $[Zn\mathbf{L}_3]_n(BF_4)_{2n}$ (a), $[Zn\mathbf{L}_3]_n(ClO_4)_{2n}$ (b), and $[Zn_2(NO_3)_4\mathbf{L}_3]_n$ (c).

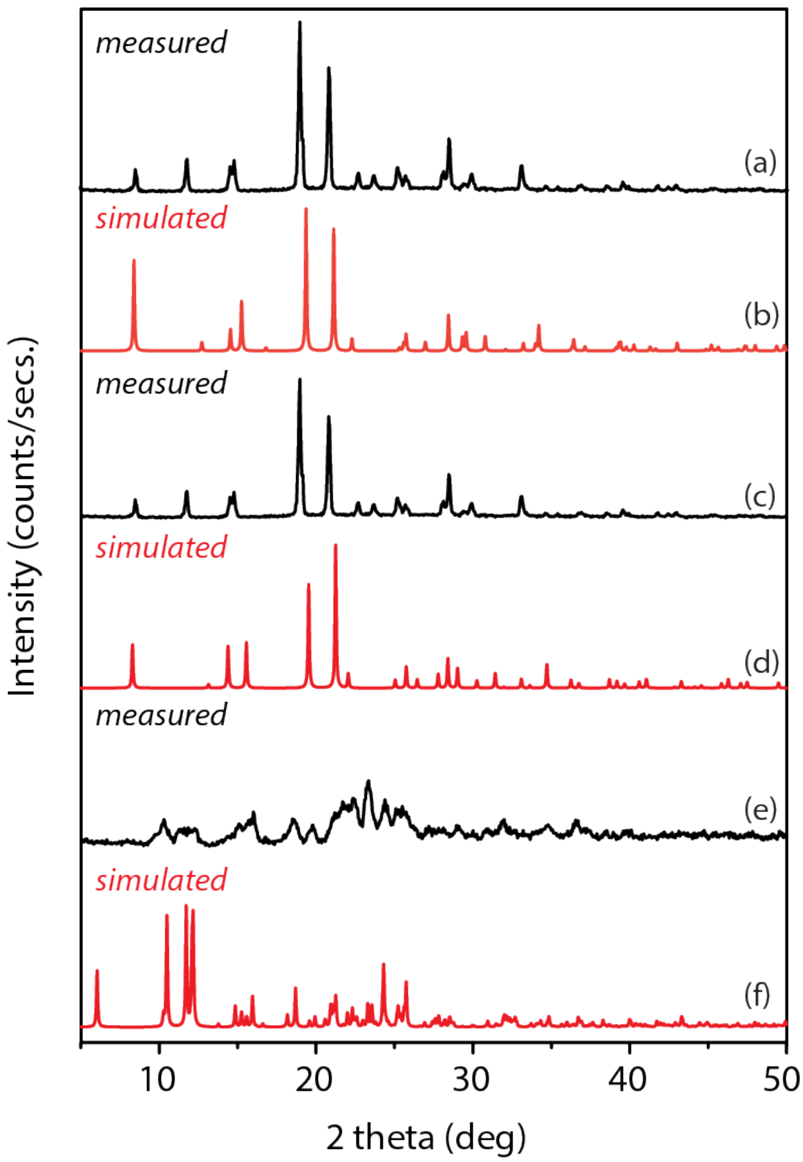

Figure S10. Powder XRD patterns for $[Zn\mathbf{L}_3]_n(BF_4)_{2n}$ (a, b), $[Zn\mathbf{L}_3]_n(ClO_4)_{2n}$ (c, d), and $[Zn_2(NO_3)_4\mathbf{L}_3]_n$ (e, f).

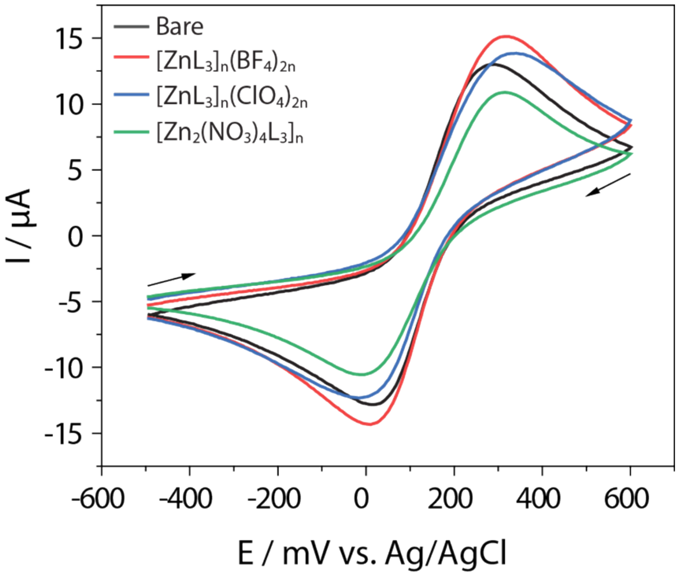

Figure S11. Electron transport behaviors of bare, $[Zn\mathbf{L}_3]_n(BF_4)_{2n}$, $[Zn\mathbf{L}_3]_n(ClO_4)_{2n}$, and $[Zn_2(NO_3)_4\mathbf{L}_3]_n$ electrodes at scan rate 50 mV s^{-1}. The $[Zn_2(NO_3)_4\mathbf{L}_3]_n$ electrode showed low electrochemical activity due to structural instability. In particular, $[Zn\mathbf{L}_3]_n(BF_4)_{2n}$ showed the highest electrochemical activity among the three zinc(II) materials, which indicates that modified on the electrode surface with $[Zn\mathbf{L}_3]_n(BF_4)_{2n}$ effectively accelerated electron transfer process between the molecules and the electrode surface.

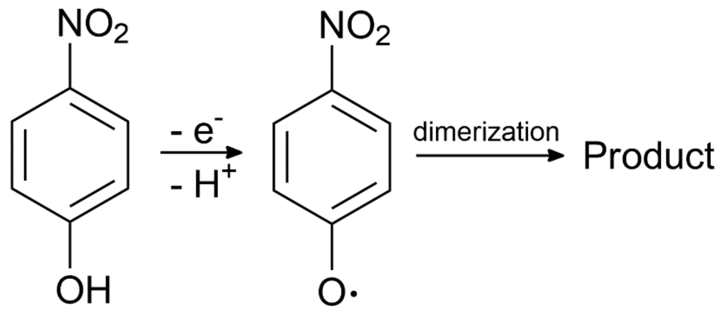

Figure S12. Proposed mechanism for 4-NP oxidation under present conditions.

Reference

1 A. L. Spek, PLATON SQUEEZE: a tool for the calculation of the disordered solvent contribution to the calculated structure factors, *Acta Crystallogr. Sect. C Struct. Chem.*, 2015, **71**, 9–18.